Key Points:
- Significant groundwater gains/losses vary over space, time, and discharge
- Karst groundwater exchanges create constant river chemistry
- Base flow is dominantly karst conduit groundwater

Supporting Information:
- Supporting Information S1

Correspondence to:
B. T. Neilson,
bethany.neilson@usu.edu

Stream Centric Methods for Determining Groundwater Contributions in Karst Mountain Watersheds

B. T. Neilson[1] (ID)**, H. Tennant[1], T. L. Stout[1], M. P. Miller[2]** (ID)**, R. S. Gabor[3,4], Y. Jameel[3,5]** (ID)**, M. Millington[3,5], A. Gelderloos[3,5], G. J. Bowen[3,5]** (ID)**, and P. D. Brooks[3,5]** (ID)

[1]Civil and Environmental Engineering, Utah Water Research Laboratory, Utah State University, Logan, UT, USA, [2]U.S. Geological Survey, Utah Water Science Center, West Valley City, UT, USA, [3]Global Change and Sustainability Center, University of Utah, Salt Lake City, UT, USA, [4]School of Environment and Natural Resources, The Ohio State University, Columbus, OH, USA, [5]Department of Geology and Geophysics, University of Utah, Salt Lake City, UT, USA

Abstract Climate change influences on mountain hydrology are uncertain but likely to be mediated by variability in subsurface hydrologic residence times and flow paths. The heterogeneity of karst aquifers adds complexity in assessing the resiliency of these water sources to perturbation, suggesting a clear need to quantify contributions from and losses to these aquifers. Here we develop a stream centric method that combines mass and flow balances to quantify net and gross gains and losses at different spatial scales. We then extend these methods to differentiate between karst conduit and matrix contributions from the aquifer. In the Logan River watershed in Northern Utah we found significant amounts of the river water repeatedly gained and then lost through a 35-km study reach. Further, the direction and amount of water exchanged varied over space, time, and discharge. Streamflow was dominated by discharge of karst conduit groundwater after spring runoff with increasing, yet still small, fractions of matrix water later in the summer. These findings were combined with geologic information, prior subsurface dye tracing, and chemical sampling to provide additional lines of evidence that repeated groundwater exchanges are likely occurring and river flows are highly dependent on karst aquifer recharge and discharge. Given the large population dependent on karst aquifers throughout the world, there is a continued need to develop simple methods, like those presented here, for determining the resiliency of karst groundwater resources.

1. Introduction

The impacts of climate change on both surface and groundwater resources are uncertain (Barnhart et al., 2016; Meixner et al., 2016). Uncertainty in predicting regional shifts in the amount, timing, and form (rain versus snow) of precipitation further complicates predictions of future water availability (Barnett et al., 2005; Harpold & Brooks, 2018). Limited knowledge of hydrologic connectivity and processes in mountainous areas further limits this understanding (Bales et al., 2006). It now is largely recognized that the majority of precipitation evaporates or infiltrates soils, acquiring distinct hydrochemical signatures that reflect groundwater flow paths and residence times before discharging as surface water (Brooks et al., 2015; Godsey et al., 2009; McIntosh et al., 2017; Miller et al., 2016). However, karst geology alters these dynamics via complex systems of conduits, caverns, and rock compositions, thereby adding another largely unquantified level of complexity in addressing questions of future water availability in karst mountain systems (Hartmann et al., 2014).

Understanding karst aquifer response to a changing climate is critical to the 20–25% of the global population dependent on karst aquifers as a water source (Ford & Williams, 2007; Hartmann et al., 2017). However, the complex nature of karst aquifers, combined with surface water basins that often do not correspond with the associated groundwater basin (Kačaroğlu, 1999; Longenecker et al., 2017), inhibits estimation of current water availability and makes the resilience of these aquifers difficult to predict. As summarized within Hartmann et al. (2014), many studies have attempted to quantify the storage and model the hydrologic connectivity within karst aquifers, but large quantities of hydrogeologic information and tracer studies are required to obtain these estimates and significant predictive uncertainty remains. Further, there is an additional need for simple methods to determine how these aquifers interact with surface waters (e.g., rivers/streams) due to the dependence on karst-fed surface waters for water supply.

In most mountainous regions, streams and rivers are fed by shallow flow paths with a larger fraction of water sourced from deeper or longer flow paths during low flow periods. In karst mountainous regions, the connectivity of the aquifer to surface waters is often in the form of easily identifiable, high discharge, karst springs

(Bogli, 1980; White, 2002). These springs are fed by macropore flows with very low residence times and high velocities (Bakalowicz, 2005; Kačaroğlu, 1999). These macropores, and karst aquifers in general, can be recharged via surface streams, diffuse infiltration, internal runoff, or overland flow from snowmelt or rain events (White, 2002). While karst conduit springs are often thought of as the dominant groundwater contributor to surface waters, there are still possible contributions or losses from other karst porosities (e.g., micropores and small fissures and fractures; Hartmann et al., 2014) and nonkarstic (porous media) sources that have much lower velocities and higher residence times. This duality in process and storage variability (Kiraly, 1998) can be classified as the matrix (i.e., high residence time) and karst conduit fractions. The velocities, flow paths, and residence times of these two fractions differ greatly and alter the respective chemical signatures (Maloszewski et al., 2002; McIntosh et al., 2017).

Quantifying the relative fraction of karst conduit and matrix groundwater contributions is critical to assessing the vulnerability, or potential for significant change, of the water source to changing precipitation regimes. Understanding groundwater contributions is particularly important in karst systems because recharge and discharge respond quickly to precipitation events or snowmelt (e.g., White, 2002) and the anticipated changes to precipitation regimes in mountainous areas will alter the recharge quantity, discharge timing, and the relative contributions of karst conduit and matrix fractions to surface waters. Further, there is a need to understand losses from a system because outflows can be critical in understanding mass fate and transport (McCallum et al., 2012) and in providing additional aquifer recharge information (Ruehl et al., 2006). In karst aquifers, these losses can also be critical to understanding the basin-scale water balance and mass fate and transport because they can result in interbasin transfers.

Given the high heterogeneity in subsurface residence times in karst systems, how do we quantify the spatial and temporal variability in groundwater exchanges with surface water at scales relevant to watershed management? To address this question, we develop a stream centric method for determining the interactions of mountainous karst aquifers with perennial rivers to quantify gross gains and losses at different spatial and temporal scales. We also provide a method to estimate the relative contributions of karst conduit and matrix groundwater contributions throughout these basins by combining flow and ion mass balances. Chemical information at relatively small spatial scales provides additional lines of evidence to support the groundwater exchange estimates throughout the study reach. These analyses can provide insight regarding losing reaches that should be protected as they recharge the aquifer and reaches with karst groundwater influences that may not have identifiable springs. They also provide information needed to determine the vulnerability of key water sources (e.g., rivers or springs) that are primarily fed by short residence time, karst conduit groundwater.

2. Materials and Methods

2.1. Study Site

The Logan River basin is centrally located in the Bear River mountain range east of Logan, Utah. With headwaters near the Utah-Idaho border, this third-order, high-gradient river flows southwest through a watershed of mostly natural land cover (forest and rangeland) with little development other than paved and dirt roads and a small number of summer homes. Currently, the majority of the precipitation falls as snow, resulting in a snowmelt-dominated hydrograph where peak flows occur in the spring with an average annual flow of approximately 6.5 m³/s. However, future climate conditions may result in more rain and less snow (Klos et al., 2014) that varies as a function of elevation (Tennant et al., 2015). The watershed is characterized by limestone and dolomite geology (Dover, 1995) and karst topography. Spangler (2001, 2011) stated that some geologic layers in Logan Canyon (e.g., Garden City Formation and Laketown Dolomite) have more karst development, but all units have the ability to transmit water via dissolution enhanced fractures, faults, and bedding planes. The exception is the Swan Peak Formation, primarily composed of quartzite, which minimizes vertical groundwater movement between some of the karst layers and intersects the river in multiple places (Figure S1 in the supporting information; Spangler, 2011). The movement of groundwater is also influenced by the Logan Peak Syncline and the Naomi Peak Syncline and Cottonwood Canyon Anticline that merge near Wood Camp Spring (Bahr, 2016; Figure S1).

There are three major karst springs that provide significant flow to the river (Rick's, Wood Camp, and Dewitt Springs, Figure 1d) throughout most of the year. There are numerous smaller springs within the basin (both karst and nonkarst) that feed the Logan River or tributaries that may or may not flow year round. Many tracer
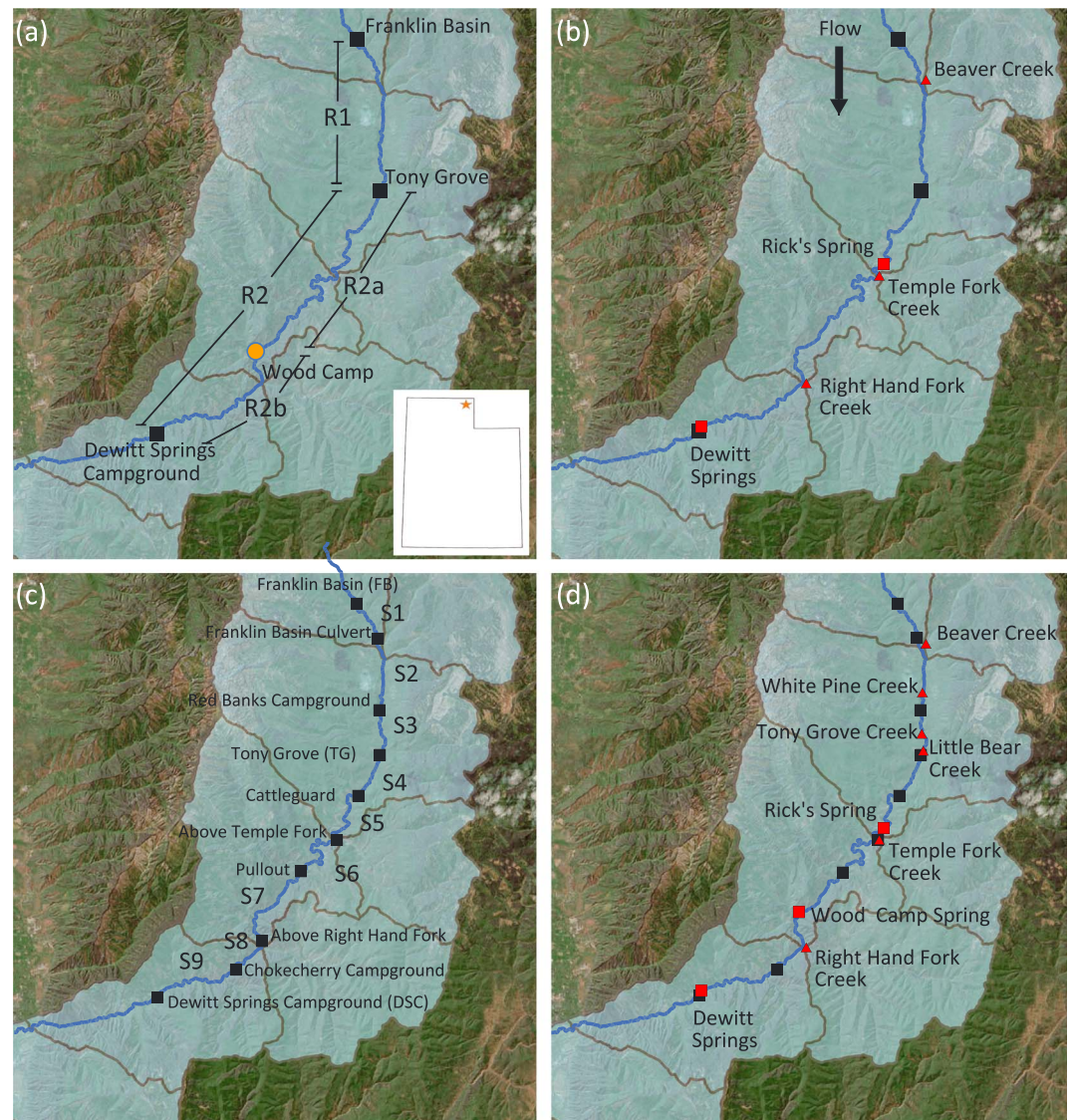
Figure 1. Gaging stations along the (a) Logan River (black squares) and within (b) major tributaries (red triangles) and karst conduit springs (red squares) for estimating $Q_{GW,Net}$ for Reach 1 (R1) and Reach 2 (R2). The orange circle represents a shorter term gaging location where $Q_{GW,Net}$ was calculated for the subreaches R2a and R2b. Synoptic gaging and chemistry sampling locations along the (c) Logan River creating nine sections (S1–S9) within the larger reaches and while accounting for the (d) major tributaries and karst conduit springs.

studies have been conducted that established subsurface connectivity of the karst aquifer and these major springs (Spangler, 2001, 2011; Figure S1) and other short residence time intrabasin and interbasin subsurface connectivity. Dewitt Spring is a primary drinking water source for Logan City, and therefore, a large portion of its flow is diverted for consumption before entering the Logan River. Similar to many karst systems, the demand for water is large. In the lower portion of the watershed demand is dominated by urban and agriculture, so that most, and sometimes all, of the flow is diverted from the river for summertime domestic, commercial, and irrigation purposes.

2.2. Field Data Collection

Streamflow and hydrochemical samples from rivers and springs connected to karst aquifers provide insight into the dynamic and spatially variable groundwater exchanges (Barberá & Andreo, 2015; Pinault et al., 2001). Flow data were collected over 3 years at long (~35 km), intermediate (~15 km), and short spatial scales (~1–5 km). Four gaging stations were established along 35 km of the main stem of the Logan River for

continuous discharge measurements. Initially, two longer reaches (Reach 1 (R1) and Reach 2 (R2)) were established in August 2015. Within Reach 2, two smaller subreaches (R2a and R2b) were established in May 2016 and data collection continued at all four sites until May 2017 (Figure 1a). To quantify perennial inflows to this study area, gaging stations were also established at the mouths of the three tributaries (Beaver Creek, Temple Fork Creek, and Righthand Fork Creek) and two of the three perennial karst conduit springs (Rick's Spring and Dewitt Spring, Figure 1b). The third karst conduit spring (Wood Camp Spring) is above the Wood Camp gaging location (Figure 1a), but has multiple complex inflow locations where rating curve development was ineffective. Summary site information and periods of data collection are provided in Table S1.

Shorter reach (~1–5-km) synoptic flow surveys were conducted in June, August, and December 2014 and June and August 2015 where flow measurements were taken at a number of locations within each reach (R1 and R2), thereby creating smaller sections (S1–S9). The flow measurements were made using velocity-area measurements with a YSI SonTek Flowtracker Handheld Acoustic Doppler Velocimeter. Flows were taken at 8–11 main stem Logan River locations (Figure 1c shows the 10 primary locations and the resulting nine sections [S1–S9]) and any tributaries or springs (using either the YSI FlowTracker or dilution gaging methods) contributing to the river at that time (Figure 1d). Note that the intermittent tributaries (White Pine Creek, Tony Grove Creek, and Little Bear Creek) were only measured when flowing and there are no major withdrawals throughout this portion of the basin. During these surveys, all flow measurements for each section (S1–S9) were collected during steady flow conditions.

During the 2015 synoptic studies, both flow and water quality were measured within the main stem Logan River and all tributaries and springs. Water quality parameters of temperature, specific conductivity, pH, and dissolved oxygen were measured in situ using a YSI 6920 V2 Sonde. Water samples were collected and filtered immediately upon collection. Samples for dissolved organic matter were filtered with precombusted 0.7-μm Whatman GF/F and collected in an acid-washed precombusted amber glass bottle. Samples for dissolved inorganic carbon (DIC) analysis (concentration and δ^{13}C) were filtered with precombusted 0.7-μm Whatman GF/F and collected in acid-washed Low Density PolyEthylene (LDPE) or High Density PolyEthylene (HDPE) bottles without headspace during the August survey. Samples for ion analysis were filtered with a 0.45-μm nylon filter into acid-washed LDPE bottles and frozen (Cl^-, SO_4^{2-}, PO_4^{3-}, NO_3^-, F^-) or acidified with nitric acid (Na^+, Mg^{2+}, Ca^{2+}, K^+, NH_4^+). Water isotope samples (δ^2H and δ^{18}O) were collected unfiltered in a glass vial with no headspace. All samples were immediately placed in coolers until transported to the lab where they were frozen or refrigerated until analysis. The analytical methods used for all samples are described within Gabor et al. (2017).

In June 2017, additional water samples were gathered from any accessible springs to get a broader understanding of the variability in spring chemistry throughout this portion of the basin. In an effort to classify these springs as karst conduit or nonkarst, we identified conservative ion (Na^+ and Cl^-) concentration ranges for springs that discharged directly from a karst conduit and had been mapped as low residence time karst features via dye tracing tests (Spangler, 2001). Using these ranges, we then classified other springs as either karst or matrix based on their respective concentration ranges and whether or not they fell within the karst Na^+ and Cl^- concentration bounds for all samples collected.

2.3. Flow and Mass Balances

To quantify the net contribution of groundwater to a section (S1–S9) or reach (R1–R2), a basic flow balance (equation (1)) was applied.

$$\Delta Q = Q_{GW,Net} = Q_2 - Q_1 - Q_{Trib} \tag{1}$$

where ΔQ is the net change in flow that can also be considered the net groundwater contribution or loss ($Q_{GW,Net}$; m^3/s), Q_2 is the flow at the downstream boundary of the section (m^3/s), Q_1 is the flow at the upstream boundary of the section (m^3/s), and Q_{Trib} is the flow contribution (m^3/s) from a tributary or measured springs. By removing the springs, net groundwater contributions highlight the contributions from other unidentified sources. Groundwater contributions can also be reported as a percent change (equation (2)).

$$\%\Delta Q = \frac{\Delta Q}{Q_1}\,(100) \tag{2}$$

where $\%\Delta Q$ is the percent change in flow relative to the upstream flow (Q_1) for the section or reach. Flow measurements taken using the velocity area method typically have errors of 3–6% (Sauer & Meyer, 1992).

To account for the combined measurement error in equation (1), following the methods of Hsieh et al. (2007), we sum the variance of each measurement, assume a 10% error in each measurement to be conservative, and determine the standard deviation of ΔQ. In this study, ΔQ values greater than ± 1 standard deviation are considered significant.

Groundwater gains and losses have been found to occur simultaneously at various scales (e.g., Ruehl et al., 2006; Schmadel et al., 2014), so the actual (or gross) groundwater contributions ($Q_{GW,In}$) can also be estimated by accounting for groundwater losses (equation (3)).

$$Q_{GW,In} = Q_2 - Q_1 - Q_{Trib} + Q_{GW,Out} \tag{3}$$

where $Q_{GW,In}$ is the total groundwater contribution in the section (m^3/s) and $Q_{GW,Out}$ is the total groundwater loss in the section (m^3/s). In this and subsequent analyses, Q_{Trib} now only includes the flow contribution (m^3/s) from tributaries. Springs are no longer explicitly removed as part of this term.

Flow and mass balances have also been combined to get groundwater gains and losses over longer reaches using various conservative and nonconservative tracers (e.g., McCallum et al., 2012). For this study, we only use conservative ions leading to a simple mass balance (equation (4)).

$$(QC)_{GW,In} = (QC)_2 - (QC)_1 - (QC)_{Trib} + (QC)_{GW,Out} \tag{4}$$

where C is the concentration of Na$^+$ or Cl$^-$ at each location.

As outlined in Cook (2013), the application of these methods assumes steady state and well-mixed (vertical and lateral) conditions within the river. To make sure we met the underlying assumptions of this approach, measurements were repeated if there were any changes in flow when moving between sections to ensure steady state conditions over the measurement period. In cases where tributaries or large springs entered the river, temperature measurements provided a means to determine where the river was laterally mixed downstream and any sampling locations included in the analysis represented completely mixed conditions. Additionally, the high gradient and coarse substrate in this river enhances lateral and vertical mixing. For the higher flow sampling in June 2015, samples were collected as far out into the channel as was safe. During August low flows, samples were collected in or near the thalweg in the center of the water column. When dealing with long reaches or using other tracers, evaporation, gas exchange, radioactive decay, and hyporheic exchange are often considered (Cook, 2013). However, because we are focusing on conservative ions and relatively short sections (Figure 1 and Table S1), we set these terms to zero. In setting the hyporheic exchange term to zero, we are assuming that the solutes entering hyporheic flow paths leave and return between locations where samples were collected.

Given the data collected during the 2015 synoptic sampling events, we combined equations (3) and (4) where C is first based on Cl$^-$ data and then Na$^+$ data. This gives us three equations where $Q_{GW,Out}$, $Q_{GW,In}$ are unknown, as are $C_{GW,Out}$ and $C_{GW,In}$ for both Cl$^-$ and Na$^+$. As a way to bracket possible concentrations of losses ($C_{GW,Out}$), similar to Payn et al. (2009) and Peterson et al. (2010), we will assume that all gains occur before a loss (in before out or IO), which provides a maximum estimate of exchanges, or all losses occur before a gain (out before in or OI), which provides a minimum estimate of exchanges. This means that $C_{GW,Out}$ is set to C_1 for OI or C_2 for IO and leaves us with four unknowns ($C_{GW,In}$ for both Cl$^-$ and Na$^+$, $Q_{GW,Out}$, and $Q_{GW,In}$). Cook (2013) discusses the need to clearly identify a groundwater end-member to determine confident estimates of groundwater exchanges. However, because we were only able to access one well at one campground in this watershed (Table S2) and most other "wells" are boxed springs, spring concentrations provided the majority of the groundwater information. Therefore, we applied the ranges of spring concentrations (based on measurements described above) as bounds for $C_{GW,In}$ for Cl$^-$ so that we could solve for the other three unknowns. We solved these equations repeatedly by incrementing $C_{GW,In}$ for Cl$^-$ by 0.1 mg/L from 0.78 to 39.4 mg/L based on the range of observed spring concentrations (Table S2) to provide a range of possible solutions. Solutions were kept where $C_{GW,In}$ for Na$^+$ were $>= 0$, $Q_{GW,Out} > 0$, and $Q_{GW,In} > 0$. An additional constraint that bounded $Q_{GW,Out}$ was necessary to keep the amount of water leaving the system to a reasonable quantity. If such a bound was not set, because both gains and losses were allowed, the river water could be entirely lost

and gained back. Because this was improbable, we determined that an upper bound on the losses must be set based on observations. We therefore set the $Q_{GW,Out}$ upper bound to 1 m^3/s or the greatest net loss observed from the net flow balances. During June 2015, however, there was one reach in which no solution was possible unless losses of greater than 3 m^3/s were allowed. Given the karst nature of the system, additional evidence suggesting large losses, longer reaches over which these exchanges can occur, and different flow paths being engaged at higher flow, these values may be reasonable and were included in the results.

2.4. Karst Conduit/Matrix Groundwater Contributions

In this watershed, karst conduit and both karst and nonkarst matrix groundwater can influence the river and differentiation between these separate groundwater contributions is important to assess vulnerabilities of the groundwater system. To do this, groundwater gains from karst conduit or "karst" groundwater and the combined influence of other karst and nonkarst matrix contributions or "matrix" groundwater are considered in a flow balance (equation (5)).

$$Q_{GW,Matrix} + Q_{GW,Karst} = Q_2 - Q_1 - Q_{Trib} + Q_{GW,Out} \tag{5}$$

where $Q_{GW,\,Matrix}$ is the matrix groundwater contribution (m^3/s) and $Q_{GW,Karst}$ is the groundwater contribution from karst conduits (m^3/s). The mass balance can also be expanded to include the contribution of mass from $Q_{GW,Karst}$ and $Q_{GW,Matrix}$ (equation (6)).

$$(QC)_{GW,Matrix} + (QC)_{GW,Karst} = (QC)_2 - (QC)_1 - (QC)_{Trib} + (QC)_{GW,Out} \tag{6}$$

When considering the flow balance (equation (5)) and the mass balance (equation (6)) that include both karst conduit and matrix effects, we now have six unknowns ($Q_{GW,Out}$, $C_{GW,Out}$, $Q_{GW,Karst}$, $C_{GW,Karst}$, $Q_{GW,Matrix}$, and $C_{GW,Matrix}$). We can set $C_{GW,Out}$ to C_1 (OI) or C_2 (IO) similar to the previous analysis. However, we cannot solve for the remaining unknowns and instead provide reasonable bounds for each unknown and systematically solve the system of equations with all the different combinations of values to provide a range of possible solutions. This was completed for both June and August 2015 synoptic sampling events for both Cl$^-$ and Na$^+$. The following criteria were applied during these calculations.

1. $C_{GW,Karst}$ is set to the minimum, maximum, or mean of measured karst spring concentrations for Cl$^-$ (Min: 0.78 mg/L, Mean:1.8 mg/L, and Max:5.39 mg/L, Table S2) and Na$^+$ (Min:0.34 mg/L, Mean:1.58 mg/L, and Max:3.01 mg/L, Table S2).
2. $C_{GW,Out}$ is set to C_1 (which assumes that all groundwater outflows occur before any inflows occur (OI)) or C_2 (all inflows occur before groundwater outflows occur (OI) to bracket the influence of mass losses to groundwater.
3. Ranges for $C_{GW,Matrix}$ are sampled incrementally by 0.1 mg/L for Cl$^-$ (5.39–50 mg/L, Table S2) and Na$^+$(3.01–50 mg/L Na$^+$, Table S2). Ranges were set as values greater than the maximum $C_{GW,Karst}$ value and lower than an arbitrary value of 50 mg/L. To account for potential variability not captured within the samples, this upper bound was set higher than the maximum observed well concentration for Cl$^-$.
4. $Q_{GW,Out}$ values are sampled at 0.02 m^3/s increments between 0 and 1 m^3/s. This upper value was set based on maximum values observed from net flow balances.

With these ranges of values, $Q_{GW,Karst}$ and $Q_{GW,Matrix}$ were solved for given all possible combinations of $C_{GW,Karst}$, $C_{GW,Out}$, $C_{GW,Matrix}$, and $Q_{GW,Out}$ for either Na$^+$ or Cl$^-$. Using all the solutions that met the criteria outlined, the associated minimum, maximum, average, and standard deviation for $Q_{GW,Matrix}$, $C_{GW,Matrix}$, $Q_{GW,Karst}$, $C_{GW,Karst,}$ and $Q_{GW,\,Out}$ were calculated for each section or groups of sections.

Because we were solving for groundwater concentrations similar to Batlle-Aguilar et al. (2014), criteria for the applicability of these approaches from Cook (2013, 2015) were tested based on the resulting $C_{GW,In}$, $C_{GW,Karst}$, and $C_{GW,Matrix}$ (see supporting information for details). Based on the initial results of these calculations, some sections (S1–S9 in Figure 1c) were combined as needed within June and August.

3. Results

3.1. Flow and Ion Trends

The study reach generally shows increasing discharge with distance downstream over both 2015 synoptic sampling efforts (Figure 2a) and other flow balance studies conducted in 2014 (Figure S2). These gains are due in part to tributaries and large karst springs (Figure 1d) joining the Logan River as well as groundwater discharge directly to the river. The ion data corresponding to all flow measurements (Figures 2b–2f) show relatively constant values along the Logan River, even though inflow concentrations from tributaries and springs vary. Due to significant contributions from karst springs and dominant limestone and dolomite bedrock, Mg^{2+} and Ca^{2+} concentrations average 15.7 ± 1.5 mg/L and 49.7 ± 1.8 mg/L, respectively, within the main stem (Figures 2d and 2e). However, the tributaries and springs often have higher concentrations (18.5 ± 3.1 mg/L and 53.5 ± 7.3 mg/L, respectively). Both Na^+ and Cl^- are assumed to be conservative and show minimal longitudinal variability along the main stem (e.g., August $Na^+ = 2.4 \pm 0.5$ and $Cl^- = 2.7 \pm 0.8$) for sections S3–S9 shown in Figure 1c. The exception is S7 at the Above Right Hand Fork Creek sampling location (see Figure 1c) where Cl^-, Na^+, and SO_4^{2-} concentrations were lower during one or both of the sampling efforts. The tributaries show significant variability in Na^+ and Cl^- with concentrations in some 2 to 3 times higher than the main stem. While the influence of these tributaries on the main stem chemistry is often unobservable, those locations where main stem concentrations do change are quickly reset downstream to the upstream main stem concentrations. In the upper portion of the watershed (S1–S2), there can be some variability in Ca^{2+} and Mg^{2+} in June and Na^+ and Cl^- are lower for both sampling periods. SO_4^{2-} is nearly constant along the study reach during both sampling efforts, and there was similar longitudinal consistency for other ions (Figure S3).

The data collected from various springs throughout 2015–2017 provided insight regarding the temporal and spatial variability of their influence. Each of the large karst springs sampled during the synoptic efforts shows some variability in ion concentrations over time with larger variability between the springs (Figures 2b–2f shown as squares). However, when considering the range of Na^+ and Cl^- concentrations for all springs sampled, the karst spring spatial and temporal variability is relatively limited with consistently low concentrations (Figure 3 and Table S2). The one exception is a sample from January 2016 from Rick's Spring during a time when the sample was collected from the nearly stagnant pool at the spring outlet and both Na^+ and Cl^- concentrations were anomalously high. Outside of these measurements, there is a clear delineation of karst ($Na^+ = 0.34$–3.01 mg/L, $Cl^- = 0.78$–5.39 mg/L) versus nonkarst springs ($Na^+ > 3.02$ mg/L, $Cl^- > 5.4$ mg/L) for Na^+ and Cl^- (Figure 3) that was not consistent or easily defined for Ca^{2+}, Mg^{2+}, and SO_4^{2-} (Figure S4).

3.2. Flow and Mass Balances

3.2.1. Long- and Intermediate-Reach Length Discharge Patterns

To begin understanding the hydrologic exchanges throughout the study reach, the longer reach net flow balances show R1 (Figure 1a) to consistently gain ~0.74 m^3/s during times of the year when snowmelt and spring runoff are not occurring (Figure 4a). During spring runoff, the net gain in flow over the reach is significant and in part due to the intermittent tributaries that flow during this period. We expect that these intermittent tributaries are largely fed by short groundwater flow paths that are activated during periods of snowmelt and significant rainfall. In contrast to R1, R2 shows variable gain and loss patterns during lower flow periods. Late summer 2015 showed gaining conditions that transitioned to losing during late fall and early winter. During 2016, however, late summer conditions were losing, followed by intermittent gaining periods likely related to precipitation events. To highlight the spatial variability of groundwater gains and losses, and some of the limitations of the lower resolution but temporally variable information, a flow balance was completed on two portions of R2 (R2a and R2b, Figure 1a) for 2016. During lower flow conditions, it is clear that R2a was consistently gaining, while R2b was consistently losing even after spring runoff initiated (Figure 4b). R2 experienced a similar large increase in flow during spring runoff (Figure 4a). In this reach, the two perennial tributaries (Temple Fork and Right Hand Fork Creeks) and two major springs (Rick's and Dewitt Springs) were gaged and accounted for in these calculations (Figure 1b). However, Wood Camp Spring has multiple outlets and provides a significant amount of flow during periods of melt but was not gaged. There are also a number of other intermittent tributaries and smaller springs that contribute to this large gain in the spring.

3.2.2. Shorter-Reach Discharge Patterns

The synoptic sampling events over both 2014 and 2015 provide higher-resolution information on the spatial variability of gains and losses over different hydrologic conditions (Figure 5). The ΔQ and $\%\Delta Q$ values for all
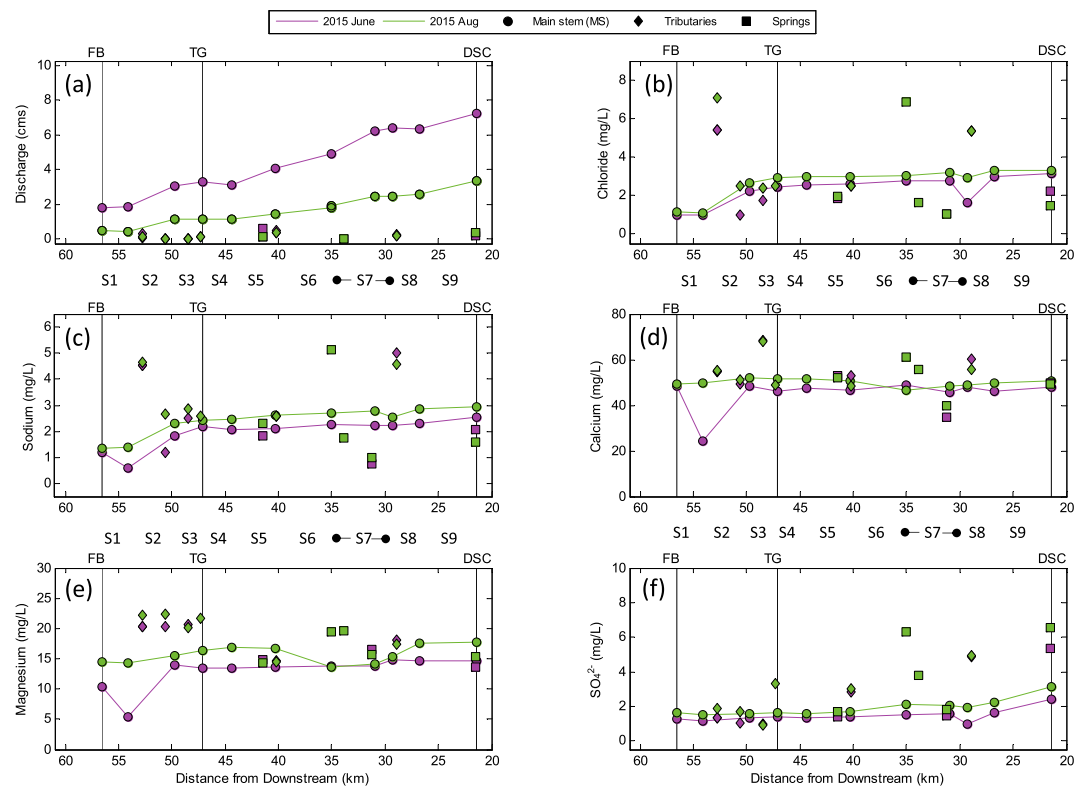
Figure 2. Discharge and ion concentrations through the study reach from June (purple) and August (green) 2015 synoptic sampling for S1–S9 (Figure 1c).

flow sampling efforts illustrate both the spatial and temporal variability of the gains and losses and the variability between years. The temporal variability is best highlighted by comparing values from a similar time period of different years. For example, June 2014 and June 2015 values for S9 transition from significantly losing to significantly gaining. This can be related in part to the timing of runoff. However, a similar pattern occurs in S5 where the reach is gaining in August 2015, but losing in August 2014. In many of the reaches, the patterns of gaining and losing are more consistent with gains or neutral conditions occurring throughout most of the sampling efforts. The exception is that S1 and S3 both experience significant net losses during August 2015. In those reaches with consistent gains, it is important to note the %ΔQ values were frequently greater than 20% of the upstream flow even after subtracting out the influence of major springs suggesting large, unidentified inputs of groundwater.

To evaluate these potential groundwater exchanges, the expanded flow (equation (3)) and mass balances for both Na$^+$ and Cl$^-$ (equation (4)) were used to estimate the total $Q_{GW,In}$, $Q_{GW,Out}$, and $C_{GW,In}$ by using all three equations. The results for IO, or the maximum estimate of exchanges, showed S2, S4–S5, S7, and S8–S9 as having significant gains in flow (Figure 6b), but the concentrations of these inflows were found to be very low (Figure S5b) in August. S3 and S6 both had much higher groundwater inflow concentrations ($C_{GW,In}$), but the inflow volumes were considered insignificant as they were less than the standard deviation. Simultaneously, there were flow losses in S2, S3, S4–S5, S7, and S8–S9. In June, all sections were gaining groundwater flow (Figure 6a), but the concentrations of these inflows were low (Figure S5a) with the exception of S8–S9. All sections were losing a significant amount of water, with S6–S7 being the largest loss (Figure 6a). Similar results were found using the assumption for OI (Figures S6 and S7) and provide the minimum estimate of exchanges. Together, these results suggest that groundwater is being exchanged via simultaneous inflows and outflows throughout the study reach, although there are generally larger gains than losses. By combining all three equations, we also found limited variability in possible solutions as shown by the low standard deviations, and for some reaches, there was only one possible solution (e.g., August 2015 S4–S5).
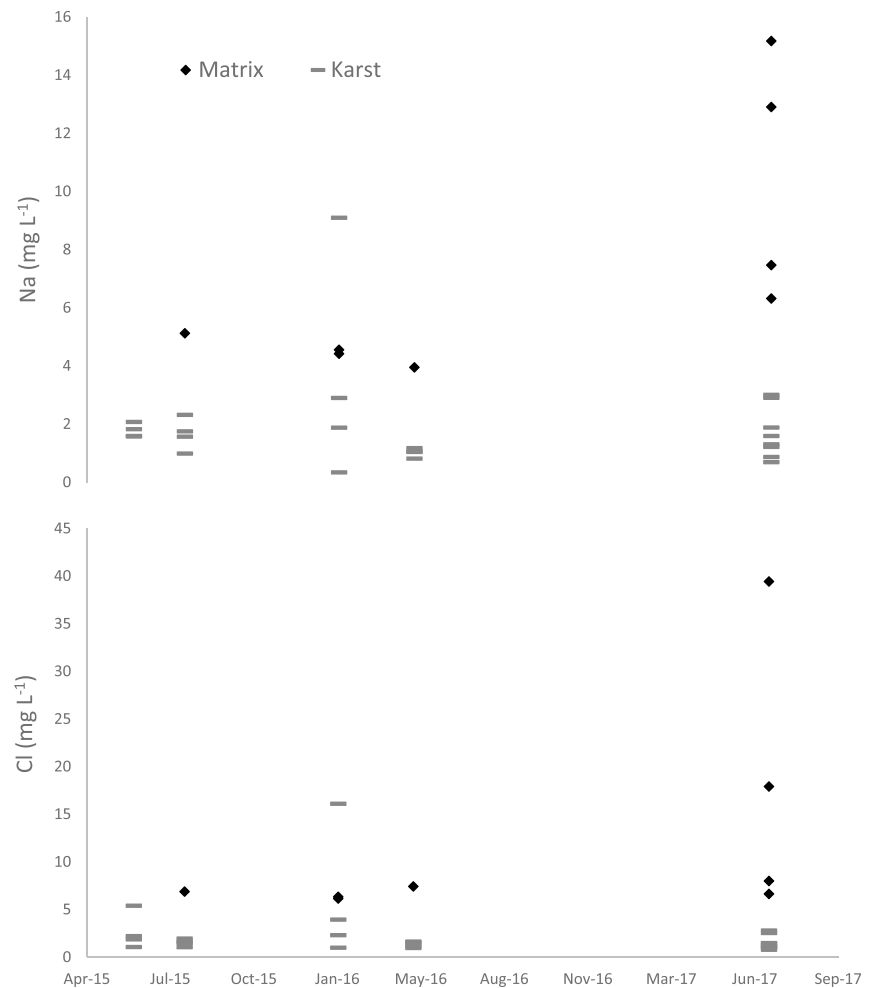
Figure 3. Sodium (Na$^+$) and chloride (Cl$^-$) concentrations from karst conduit (dashes) and matrix (diamonds) springs. High karst concentrations in January 2016 were taken from a karst spring pool that was nearly stagnant.

To ensure the applicability of these combined mass and flow balances to this system, suitability metrics provided by Cook (2013, 2015) were calculated for each reach and constituent (Na$^+$ and Cl$^-$) after the $C_{GW,In}$ values were estimated. The summary statistics (Tables S3 and S4) show that in nearly all cases, these methods meet the criteria. The exceptions were sections that had net losses (Table S4).

3.3. Karst/Matrix Groundwater Contributions

To provide further insight regarding the sources of groundwater in this watershed, we expanded the flow (equation (3)) and mass balances (equation (4)) to include both karst and matrix groundwater contributions (equations (5) and (6)). Because it was not possible to solve for all unknowns in these equations, we provided reasonable bounds for each unknown and systematically solved the system of equations with all combinations of values to provide a range of possible solutions. While there was some variability in the results when using Na$^+$ versus Cl$^-$ in the mass balance equations, each ion resulted in similar averages and standard deviations for $Q_{GW,Matrix}$, $Q_{GW,Karst}$, and $Q_{GW,Out}$ for both synoptic studies (Figures 6 and S6). Because the $Q_{GW,Matrix}$ values were all low, there was large variability in the estimated concentrations ($C_{GW,Matrix}$) due to limited mass contributions and a lack of sensitivity (Figure S5).In most reaches, the $Q_{GW,In}$ contributions estimated from all three equations were similar to $Q_{GW,Karst}$ with an overlap in the standard deviations for either Na$^+$ or Cl$^-$. The exception is S3 and S6 in August (Figure 6b) and S6–S7 in June (Figure 6a). The estimated $Q_{GW,Out}$ values were also similar among scenarios using different constituents, with the exception of S3 and S6 in August 2015 and
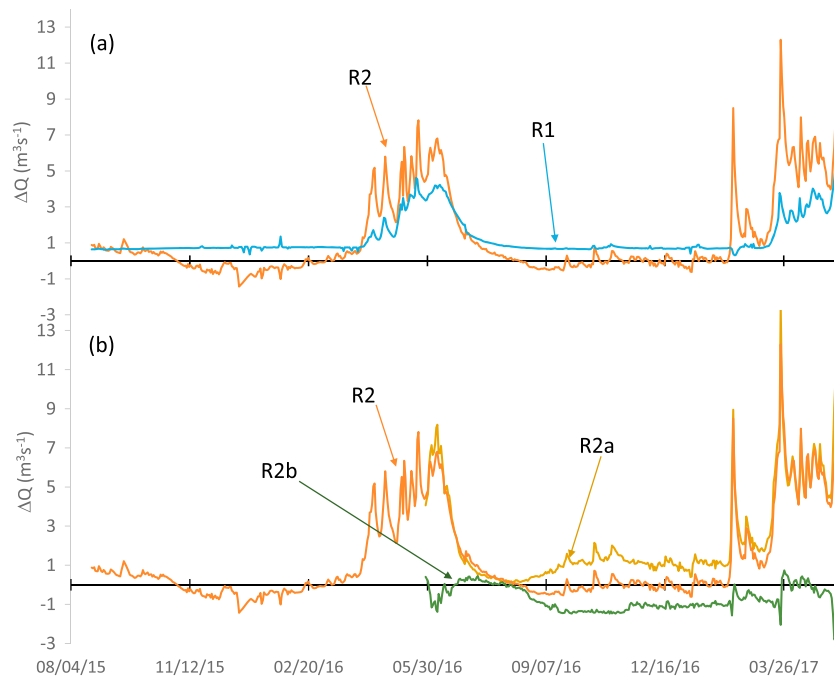
**Figure 4.** ΔQ_{Net} from flow balance for (a) R1 and R2 and (b) R2, R2a, and R2b shown in Figure 1a.

S6–S7 in June 2015. However, the 1 m^3/s constraint on $Q_{GW,Out}$ resulted only in a solution for Na^+ in the karst/matrix calculations for June S6–S7. A very large loss was estimated in this reach when using all three equations. If the bounds were relaxed for Cl^- for the karst/matrix calculations, the average $Q_{GW,Out}$ values at S6–S7 in June would range from approximately 1.5–2.5 m^3/s but result in slightly larger inflows. In this case, the results from using all three equations likely provides a more confident estimate of the exchanges, but this portion of the study area consists of complex flow paths and more information is needed to fully characterize the system. This happens to be the section that receives flow from both Rick's and Wood Camp springs, which create the high $Q_{GW,Karst}$ values, but it also spans R2b, which shows a consistent loss for much of the year (Figure 4b).

When considering the entire study reach, the concentrations of the karst contributions ($C_{GW,Karst}$) from this analysis suggest limited variability in groundwater inflow concentrations throughout the study area (Figure S5) and are consistent with the estimated concentrations ($C_{GW,In}$) from all three equations. Similar to the results from all three equations, Cook (2013, 2015) metrics were calculated for each reach and constituent (Na^+ and Cl^-) after the $C_{GW,Karst}$ and $C_{GW,Matrix}$ values were estimated (Tables S3 and S4). These calculations meet the combined flow and concentration criteria when there was a net gain. However, the ratio of $C_{GW,Karst}$ to concentrations in the main channel was often less than 1 due to dominant karst contributions.

3.4. Isotope and Carbon Trends

Other chemical measures provide additional information regarding the groundwater exchanges in this basin. DOC concentrations are low (0.76 ± 0.09 mg/L) and constant throughout the reach (Figure 7b). $\delta^{13}C$ of DIC values of the main stem also show a generally consistent pattern (Figure 7d). However, similar to ion concentrations, the tributaries can have higher DOC and DIC concentrations and elevated $\delta^{13}C$ (Figure 7).

Longitudinally similar values of $\delta^{18}O$ (Figure 7c) and d-excess (Figure 7e) also were present along the main stem for each synoptic event. The only variability in d-excess is due to the evaporated signal (i.e., lower d-excess and higher $\delta^{18}O$) of inflow from most tributaries and one spring in August. Consistent with the
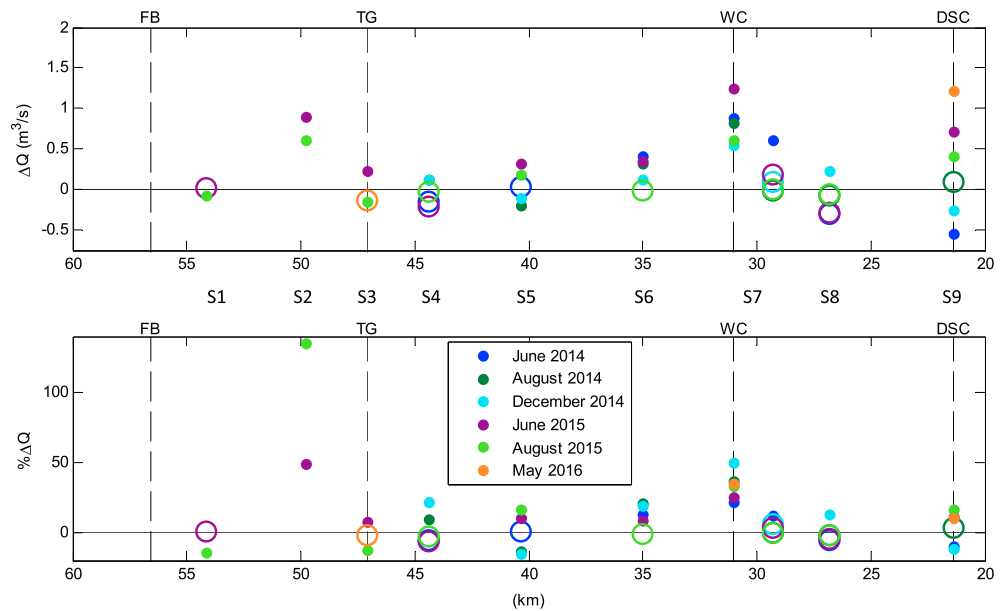
Figure 5. ΔQ and %ΔQ from synoptic flow balance S1–S9 (Figure 1c) where open circles are values that are not significantly different than zero (within one ± standard deviation of ΔQ assuming a 10% measurement error). These calculations take out all measured springs to highlight which reaches have significant gains or losses in addition to springs flowing directly into the river.
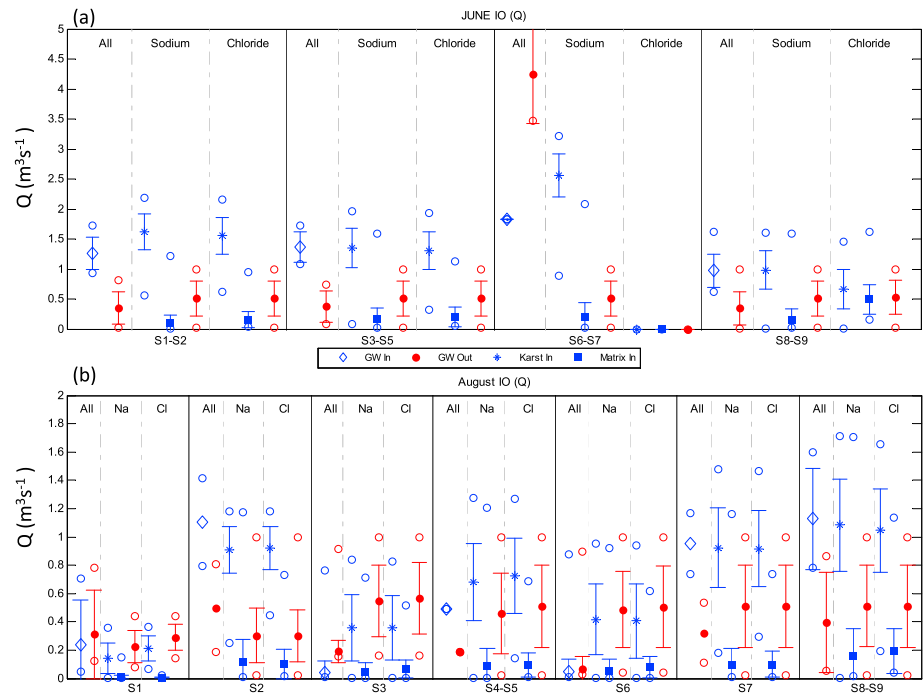
Figure 6. (a) June and (b) August 2015 estimates of $Q_{GW,In}$ and $Q_{GW,Out}$ solving all three equations together (flow balance, Na$^+$ mass balance, and Cl$^-$ mass balance, labeled All) for S1–S9 and ranges of $Q_{Karst,In}$, $Q_{Matrix,In}$, and $Q_{GW,Out}$ results for sodium (Na$^+$) and chloride (Cl$^-$) assuming that gains occur before a loss (or IO). The red color indicates different estimates of groundwater losses ($Q_{GW,Out}$), and blue indicates estimates for different inflows ($Q_{GW,In}$, $Q_{Karst,In}$, and $Q_{Matrix,In}$). Different symbols (filled circle, square, asterisk, and diamond) represent average values of all solutions that met the established criteria. Hollow circles are the associated minimum and maximum values, and error bars represent the standard deviation.
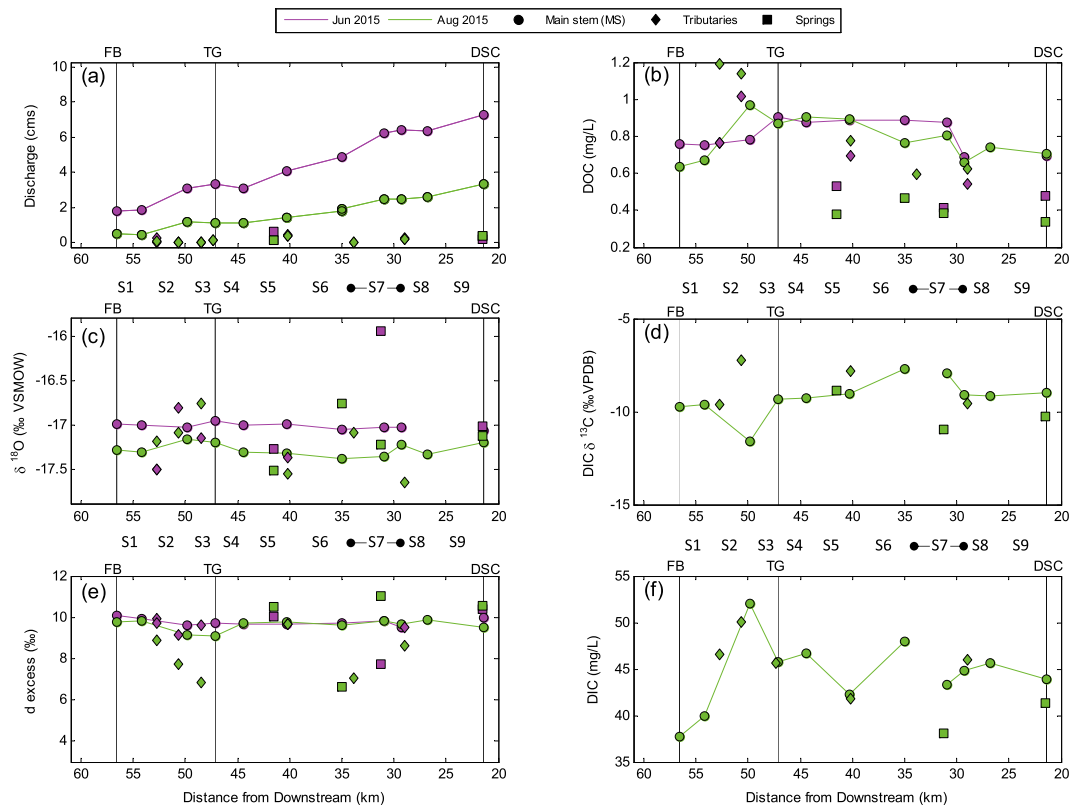
Figure 7. Plot of (a) discharge, (b) dissolved organic carbon (DOC), (c and e) water isotopes, and (d and f) dissolved inorganic carbon (DIC) for S1–S9 (Figure 1c) from June (purple) and August (green) synoptic sampling.

findings above, the influence of tributaries and springs is short lived within the main stem, and isotope values are reset a short distance downstream from sites of inflow.

4. Discussion

In recent decades, the close link between groundwater and surface water in areas of karst geology is commonly acknowledged (e.g., White, 2002). However, the difficulty associated with quantifying these exchanges (e.g., Winter, 1995) has limited our understanding of this connectivity. More recently, the dependence of surface water discharge on groundwater has been recognized in a much broader range of geologic settings (Brooks et al., 2015; Godsey et al., 2009; Kirchner, 2009). However, karst aquifers are a unique environment. In karst basins, precipitation recharges both the slower responding matrix and the faster responding karst conduit groundwater system resulting in a continuum of contributions spanning primarily karst conduit to primarily matrix (e.g., Rimmer & Salingar, 2006). The fast response of the karst system to changes in hydrology suggests that surface water flows will be more sensitive to short term fluctuations in recharge than matrix dominated systems. Further, because karst aquifers are easily polluted, provide critical water sources, and may be greatly depleted via over exploitation (Kačaroğlu, 1999), we need new methods for understanding the resiliency of these resources via an understanding of groundwater-surface water exchanges and the contribution of karst conduit versus matrix discharge.

4.1. Spatial Patterns in Discharge and Chemistry

A net increase in flow of 3.5 times (June 2015) and 6.5 times (August 2015) over the study period due to tributaries, springs, and subsurface inflows did not notably alter ion concentrations (Figure 2) in the main stem even though the inflow concentrations were often different than the river. The main stem chemostasis suggests that the dominant water source throughout the watershed is chemically consistent over space with

limited variability between June 2015 and August 2015. However, the consistently higher ion concentrations in August suggest a slight shift in this source water that may contain a greater fraction of matrix groundwater. The combined results from the flow and mass balances suggest limited matrix groundwater contributions throughout the study area, with the exception being small tributaries in the upper reaches.

Na^+ and Cl^- data from the various springs ($n = 14$) or the one available well show a relatively clear distinction between dominantly karst conduit source water and dominantly matrix source water (Figure 3 and Table S2). For example, Wood Camp Spring was sampled five times (June 2015, August 2015, February 2016, May 2016, and July 2017) resulting in a mean concentration of 0.89 ± 0.46 mg/L for Na^+ and 0.97 ± 0.11 mg/L for Cl^-. The low concentrations suggest limited matrix interactions during recharge and chemistry that looks more like surface water than groundwater (White, 2002). Dewitt Springs, Logan City's primary drinking water source, was sampled four times and has slightly higher and more variable concentrations of 1.9 ± 0.79 mg/L Na^+ and 2.3 ± 1.16 mg/L Cl^- (Table S2) but still suggests dominantly karst conduit contributions given the low concentrations. Spangler (2011) states that recharge to this karst aquifer is due primarily to snowmelt via sinkholes and pits at high elevations and distributed contributions from losing low order tributaries. However, this study also suggested that recharge via direct infiltration of diffuse fracture pathways was a substantial storage component that helped maintain high base flow in the major karst conduit springs. While the non-karst springs were not sampled as frequently, those with repeat samples (Temple Fork Spring and Pullout Spring) are relatively consistent with concentrations ranging from 3.95 to 5.1 mg/L Na^+ and 6.16–7.44 mg/L Cl^- (Table S2). The higher concentrations suggest added matrix influence, but they are still likely dominated by karst conduit flow given that the one deep well available for sampling that should represent matrix flow (Red Banks Well) shows concentrations of 12.9 mg/L Na^+ and 39.4 mg/L Cl^-. It is important to note that while we create a clear divide between dominantly karst conduit and dominantly matrix influence on these springs, all springs consist of flow contributions from both matrix and karst portions of the aquifer.

Constant DOC, $\delta^{13}C$ of DIC, $\delta^{18}O$, and d-excess values along the Logan River suggest a chemically constant groundwater source that is resetting the system frequently enough to limit chemical alteration over the 30-km study reach. In other words, a substantial fraction of the river is repeatedly turned over via simultaneous gains and losses along the study reach. The constant DOC concentrations and very low average DOC concentrations from the springs (0.31 ± 0.18 mg/L; Figure 7b) suggest that groundwater is diluting any possible increases in DOC from autochthonous production or allochthonous inputs in matrix flow. Stream DIC concentration and isotope values are governed by a variety of sources and sinks including biogenic and geogenic sources, CO_2 evasion, and in-stream processes (Campeau et al., 2017). $\delta^{13}C$ values of DIC provide important information on the source of stream DIC, where low $\delta^{13}C$ values indicate organic sources and high values can reflect CO_2 evasion and/or geogenic sources. The constant $\delta^{13}C$ values of DIC along the main stem suggest relatively limited in-stream CO_2 degassing (Doctor et al., 2008) and are consistent with DIC derived dominantly from carbonate weathering ($\delta^{13}C$ of 0 ‰) using soil CO_2 ($\delta^{13}C$ of -24 ‰) as the acid source (Figure 7d). Consistent values of $\delta^{18}O$ (Figure 7c) and d-excess (Figure 7e) show groundwater flow paths dominate streamflow because one would anticipate an increase in evaporation leading to higher $\delta^{18}O$ and/or lower d-excess in August if surface flow paths were dominant (Brooks & Lemon, 2007). Together, these chemical measures show there is a chemically constant groundwater source that is resetting the system frequently enough to limit chemical alteration over the 30-km study reach. In other words, they suggest that a substantial fraction of the river is repeatedly turned over via simultaneous gains and losses along the study reach.

4.2. Flow and Mass Balances

The flow and mass balances both show significant variability of exchanges at different scales. At the reach scale (Figure 4a), net gains are significant during spring runoff (R1 and R2) and constant during base flow (R1). However, similar to the variability of gains and losses found by Cholet et al. (2017), these longer reaches can alternate between gaining and losing conditions (e.g., R2). Such findings highlight the need to understand karst aquifer exchanges over shorter reaches to inform resource management and policy (Rugel et al., 2016). In this case, the higher-resolution subreach-scale data for R2a and R2b (Figure 1a) show a gaining upper portion (R2a) and a losing lower portion (R2b). This transition from gaining to losing occurs where the Naomi Peak Syncline and Cottonwood Canyon Anticline converge and the river elevation is lower than the impermeable Swan Peak Formation that inhibits vertical groundwater transport or karst conduit

development (Spangler, 2011). Downstream of R2a, the surficial geology becomes dominated by various dolomite formations (Dover, 1995) where karst development can contribute groundwater to or divert surface water from the river. These findings highlight the importance of geologic structure in groundwater movement (vertically and laterally) in these karst aquifers and the influence on exchanges with surface water.

Net gains and losses in flow at the higher spatial resolution further illustrate the temporal and spatial variability in exchanges as they are a function of both time of year and base flow levels (Figure 5). In some areas, there are relatively consistent net gains (e.g., S2, S6, and S7) with no consistent net losses. In some reaches, however, there is a switch from gaining to losing between different years (e.g., S5 and S9). June 2015 flows were higher than those in June 2014 (Figure S2), but August 2015 flows were lower than August 2014 due in part to very low precipitation during the spring and summer of 2015. Regardless of the general differences between 2014 and 2015, the flows at the end of S5 and S9 in August 2014 and 2015 are nearly identical. Both of these reaches have a karst spring near the end of the section, suggesting that areas near these springs create some consistency in flow at the downstream location. However, the upstream discharge of these sections was lower in the drier summer of 2015, creating the transition from gaining to losing. It is also important to note that while other calculations have not taken out the influence of the springs, these ΔQ values have removed all measured springs to illustrate the importance of groundwater gains occurring in addition to these major spring inflows. These findings suggest that higher-frequency estimates of groundwater exchanges at these scales would provide insight regarding the relationship between river flow and connectivity with the aquifer.

McCallum et al. (2012) stated that flow and mass balances can only be applied to get groundwater gains and losses when groundwater end member concentrations are known and cannot be applied to shorter reaches. However, when using all three equations (i.e., flow and Na^+ and Cl^- mass balances), our results address these concerns by determining groundwater concentrations that are generally higher than those in stream (Table S3) and meet other metrics addressing these concerns that are provided by Cook (2013, 2015; Table S4). This is not as consistent when estimating these metrics for karst contributions ($C_{GW,Karst}$). However, the results are commonly confirmed when compared to groundwater exchanges from all three equations.

The mass and flow balance analysis that differentiated karst conduit and matrix fractions suggests dominant karst contributions (Figures 6 and S5–S7) with limited matrix influence and is consistent with the inferences gained from the chemistry data. In August, the percent contribution from the matrix fraction can be slightly higher (Table 1). S9 in August also showed the greatest contributions, and this is consistent with this site being colocated with the Logan Peak Syncline intersecting the river. S2 also shows high karst conduit contributions, but there is no clear geologic explanation for it. The increase in matrix influences in August would be consistent with the karst conduit portion of the aquifer being recharged by matrix water as the more direct snowmelt recharge was discharged earlier in the summer. The increased contributions of this longer residence time, matrix water are also suggested by the increased Na^+ and Cl^-. While both the karst conduit and matrix values represent a snowmelt signal in both June and August, it is possible that the matrix recharge occurred during late season snowmelt when $\delta^{18}O$ values are lower (Taylor et al., 2001) and the superficial soils were thawed. These findings provide additional evidence of Spangler's (2001) suggested influence of lower porosity recharge providing late summer base flow to springs and the river. We anticipate that during snowmelt or times of significant precipitation, the variability in groundwater exchanges would exceed the summer, post runoff conditions measured here.

Importantly, our data suggest that these karst systems exhibit a fundamentally different response to seasonal patterns in precipitation input. In many watersheds, the fastest hydrologic responses associated with runoff events correspond with the greatest variability in chemistry (e.g., Kirchner, 2003). In contrast, we see that the dominant contributions of the "fast" flow (karst conduit contributions, Table 1) created a chemically homogeneous response throughout the system, which was only slightly altered later in the year. Further, it was the slower flow (matrix flow) in this watershed that created the limited hydrochemical variability observed later in the season. In most other basins, these older, slow response waters are typically defined as endmembers due to their consistent concentrations.

Beyond the relatively constant groundwater source waters, these calculations and the longitudinal ion, DOC, and isotope patterns suggest that in contrast to Hensley and Cohen (2012), a significant amount of water is turned over multiple times throughout the study reach via the large karst gains and losses. If the groundwater

Table 1

Estimated Average Karst Contributions as a Percentage of the Total Inflow of Groundwater ($Q_{GW,Karst} + Q_{GW,Matrix}$) and as a Percentage of the Upstream Flow (Q_1) for Each Section

Section	SITE	Δx (km)	Q_1 (m³/s)	$Q_{GW,In}$ (m³/s)	% $Q_{Karst,In}$ of $Q_{GW,In}$ sodium	% $Q_{Karst,In}$ of $Q_{GW,In}$ chloride	% $Q_{Karst,In}$ of Q_1 sodium	% $Q_{Karst,In}$ of Q_1 chloride
15 Aug								
S1	FBG-FC	2.39	0.52	0.15	93%	98%	27%	40%
S2	FC-RBC	4.03	0.45	1.03	89%	90%	203%	205%
S3	RBC-TGG	2.95	1.18	0.40	89%	84%	30%	30%
S4–S5	TGG-ATF	6.82	1.16	0.77	88%	88%	59%	62%
S6	ATF-PO	5.22	1.47	0.47	89%	84%	28%	28%
S7	PO-ARF	5.61	1.83	1.02	91%	90%	48%	48%
S8–S9	ARF-DSC	7.7	2.46	1.24	87%	84%	44%	43%
15 Jun								
S1–S2	FBG-RBC	6.42	1.83	1.71	94%	91%	88%	85%
S3–S5	RBC-ATF	9.77	3.08	1.51	89%	86%	44%	43%
S6–S7	ATF-ARF	10.83	4.08	2.76	93%	-	63%	-
S8–S9	ARF-DSC	7.7	6.38	1.14	86%	57%	15%	10%

source is consistent throughout, any in-stream processing or cumulative influences of tributaries would be minimized and result in consistent chemistry over time and space, similar to what we observed in this study. Given the complexity of this system and the variety of karst features that can develop in karst terrains, these types of exchanges are feasible. However, this study leaves questions regarding time variable karst and matrix recharge and discharge, the total size of groundwater storage, and the fate of the estimated groundwater losses. As suggested by Spangler (2001), recharge is occurring throughout the watershed via sinkholes, pits, fluvioglacial deposits, and more diffuse pathways. In many basins there is a clear relationship between snow water equivalent and base flow (e.g., Godsey et al., 2014). A similar relationship has been suggested for the Logan River by Spangler (2011); however, it is unclear how a shift in climate will influence the relative karst and matrix contributions with more rain and less snow accumulation. Regardless, this analysis suggests that the dominance of karst conduit groundwater influences on the Logan River makes it susceptible to changes in recharge from changing precipitation regimes and the short residence times of these systems would translate into relatively fast changes in the water available in karst springs or the river.

Others have established the relative importance of groundwater and surface water interactions in high-elevation catchments (Liu et al., 2004), but this study highlights the significance of these exchanges in a karst, mountain watershed. Water sourced from the entire watershed can directly impact all downstream uses due to very short karst conduit travel times (Spangler, 2001). Kačaroğlu (1999) emphasized the need for communities in karst basins to understand the vulnerability of their water sources and understand the highly connected nature of these basins as a critical component of water source protection. In the context of karst mountainous systems in the Intermountain West, it is important to understand that land uses such as grazing, forestry practices (logging and fire control), and mining in remote areas of these basins still have the opportunity to directly and adversely affect our water sources via runoff to sinkholes or other karst features that connect the land surface to the karst conduit system. This is particularly important in areas like the Logan River where karst springs are used as a primary drinking water source. In river reaches with significant losses, this aquifer recharge provides another direct connection between surface water and the groundwater system. Any accidents or spills near or in rivers parallel with high traffic corridors would influence the surface water system but could also become a source of aquifer contamination.

5. Conclusions

The direct link between snowmelt and precipitation to karst aquifer recharge and discharge requires an understanding of the karst conduit and matrix contributions to surface waters under current and future climate conditions. By applying simple methods centered on surface water sampling, we illustrate the groundwater dominance and exchange variability over time at the long (reach), intermediate (subreach), and shorter (section) scales. While some portions of the study reach show consistent gains, there are sections that switch

between gaining and losing between years due to differing base flow conditions. The spatial variability observed is also influenced by geologic controls (e.g., confining layers and synclines) and karst development. Regardless of the variability, both gains and losses occurred in nearly all portions of the study area. By combining mass and flow balances and determining karst conduit and matrix contributions, the dominant role of karst conduit discharge with increasing influences of matrix contributions later in the summer season was also established. Prior tracer work in this area and many chemical measures (e.g., ions, stable isotopes of water, δ^{13}C-DIC, and DOC) provide additional lines of evidence suggesting significant karst groundwater influences. The chemistry data support that there is a relatively constant source water with low Na^+, Cl^-, and DOC concentrations that resemble karst conduit water and create consistent longitudinal chemistry across nearly all chemical measures. The dominance of and exchanges with this source water limits the influences of tributaries and springs that chemically differ from the main stem.

The dominance of karst contributions combined with the direct response of discharge to snow pack conditions suggests significant water source vulnerability with changing precipitation patterns and the anticipation of less snow and greater rain. Additionally, the consistent gains and losses occurring throughout the study reach suggest a greater risk of both river and aquifer contamination via land uses in remote portions of the watershed or via losses from the river to other portions of the aquifer or neighboring basins.

References

Bahr, K. (2016). *Structural and lithological influences on the Tony Grove Alpine Karst System* (p. 242). Bear River Range, North Central Utah: Utah State University.

Bakalowicz, M. (2005). Karst groundwater: A challenge for new resources. *Hydrogeology Journal*, *13*(1), 148–160. https://doi.org/10.1007/s10040-004-0402-9

Bales, R. C., Molotch, N. P., Painter, T. H., Dettinger, M. D., Rice, R., & Dozier, J. (2006). Mountain hydrology of the western United States. *Water Resources Research*, *42*, W08432. https://doi.org/10.1029/2005WR004387

Barberá, J. A., & Andreo, B. (2015). Hydrogeological processes in a fluviokarstic area inferred from the analysis of natural hydrogeochemical tracers. The case study of eastern Serranía de Ronda (S Spain). *Journal of Hydrology*, *523*, 500–514. https://doi.org/10.1016/j.jhydrol.2015.01.080

Barnett, T. P., Adam, J. C., & Lettenmaier, D. P. (2005). Potential impacts of a warming climate on water availability in snow-dominated regions. *Nature*, *438*(7066), 303–309. https://doi.org/10.1038/nature04141

Barnhart, T. B., Molotch, N. P., Livneh, B., Harpold, A. A., Knowles, J. F., & Schneider, D. (2016). Snowmelt rate dictates streamflow. *Geophysical Research Letters*, *43*, 8006–8016. https://doi.org/10.1002/2016GL069690

Batlle-Aguilar, J., Harrington, G. A., Leblanc, M., Welch, C., & Cook, P. G. (2014). Chemistry of groundwater discharge inferred from longitudinal river sampling. *Water Resources Research*, *50*, 1550–1568. https://doi.org/10.1002/2013WR013591

Bogli, A. (1980). *Karst hydrology and physical speleology*. Berlin: Springer-Verlag.

Brooks, P. D., Chorover, J., Fan, Y., Godsey, S. E., Maxwell, R. M., McNamara, J. P., & Tague, C. (2015). Hydrological partitioning in the critical zone: Recent advances and opportunities for developing transferable understanding of water cycle dynamics. *Water Resources Research*, *51*, 6973–6987. https://doi.org/10.1002/2015WR017039

Brooks, P. D., & Lemon, M. M. (2007). Spatial variability in dissolved organic matter and inorganic nitrogen concentrations in a semiarid stream, San Pedro River, Arizona. *Journal of Geophysical Research*, *112*, G03S05. https://doi.org/10.1029/2006JG000262

Campeau, A., Wallin, M. B., Giesler, R., Löfgren, S., Mörth, C.-M., Schiff, S., et al. (2017). Multiple sources and sinks of dissolved inorganic carbon across Swedish streams, refocusing the lens of stable C isotopes. *Scientific Reports*, *7*(1), 9158. https://doi.org/10.1038/s41598-017-09049-9

Cholet, C., Charlier, J. B., Moussa, R., Steinmann, M., & Denimal, S. (2017). Assessing lateral flows and solute transport during floods in a conduit-flow-dominated karst system using the inverse problem for the advection–diffusion equation. *Hydrology and Earth System Sciences*, *21*(7), 3635–3653. https://doi.org/10.5194/hess-21-3635-2017

Cook, P. G. (2013). Estimating groundwater discharge to rivers from river chemistry surveys. *Hydrological Processes*, *27*(25), 3694–3707. https://doi.org/10.1002/hyp.9493

Cook, P. G. (2015). Quantifying river gain and loss at regional scales. *Journal of Hydrology*, *531*(Part 3), 749–758.

Doctor, D. H., Kendall, C., Sebestyen, S. D., Shanley, J. B., Ohte, N., & Boyer, E. W. (2008). Carbon isotope fractionation of dissolved inorganic carbon (DIC) due to outgassing of carbon dioxide from a headwater stream. *Hydrological Processes*, *22*(14), 2410–2423. https://doi.org/10.1002/hyp.6833

Dover, J. H. (1995). Geologic map of the Logan 30'x60' quadrangle, Cache and Rich Counties, Utah, and Lincoln and Uinta Counties, Wyoming, U.S. Geological Survey.

Ford, D. C., & Williams, P. W. (2007). *Karst hydrogeology and geomorphology*. Chichester, UK: Wiley. https://doi.org/10.1002/9781118684986

Gabor, R. S., Hall, S. J., Eiriksson, D. P., Jameel, Y., Millington, M., Stout, T., et al. (2017). Persistent urban influence on surface water quality via impacted groundwater. *Environmental Science & Technology*, *51*(17), 9477–9487. https://doi.org/10.1021/acs.est.7b00271

Godsey, S. E., Kirchner, J. W., & Clow, D. W. (2009). Concentration–discharge relationships reflect chemostatic characteristics of US catchments. *Hydrological Processes*, *23*(13), 1844–1864. https://doi.org/10.1002/hyp.7315

Godsey, S. E., Kirchner, J. W., & Tague, C. L. (2014). Effects of changes in winter snowpacks on summer low flows: Case studies in the Sierra Nevada, California, USA. *Hydrological Processes*, *28*(19), 5048–5064. https://doi.org/10.1002/hyp.9943

Harpold, A., & Brooks, P. D. (2018). Humidity determines snowpack ablation under a warming climate. *Proceedings of the National Academy of Sciences*, *115*(6), 1215–1220. https://doi.org/10.1073/pnas.1716789115

Hartmann, A., Gleeson, T., Wada, Y., & Wagener, T. (2017). Enhanced groundwater recharge rates and altered recharge sensitivity to climate variability through subsurface heterogeneity. *Proceedings of the National Academy of Sciences*, *114*(11), 2842–2847. https://doi.org/10.1073/pnas.1614941114

Hartmann, A., Goldscheider, N., Wagener, T., Lange, J., & Weiler, M. (2014). Karst water resources in a changing world: Review of hydrological modeling approaches. *Reviews of Geophysics*, *52*, 218–242. https://doi.org/10.1002/2013RG000443

Hensley, R. T., & Cohen, M. J. (2012). Controls on solute transport in large spring-fed karst rivers. *Limnology and Oceanography*, *57*(4), 912–924. https://doi.org/10.4319/lo.2012.57.4.0912

Hsieh, P. A., Barber, M. E., Contor, B. A., Hossain, M. A., Johnson, G. S., Jones, J. L., & Wylie, A. H. (2007). *Ground-water flow model for the Spokane Valley-Rathdrum prairie aquifer* (p. 78). Spokane County, Washington, and Bonner and Kootenai counties, Idaho, U.S. Geological Survey.

Kačaroğlu, F. (1999). Review of groundwater pollution and protection in karst areas. *Water, Air, and Soil Pollution*, *113*(1/4), 337–356. https://doi.org/10.1023/A:1005014532330

Kiraly, L. (1998). Modeling karst aquifers by the combined discrete channel and continuum approach. *Bulletin d'Hydrogeologie*, *16*, 77–98.

Kirchner, J. W. (2003). A double paradox in catchment hydrology and geochemistry. *Hydrological Processes*, *17*(4), 871–874. https://doi.org/10.1002/hyp.5108

Kirchner, J. W. (2009). Catchments as simple dynamical systems: Catchment characterization, rainfall-runoff modeling, and doing hydrology backward. *Water Resources Research*, *45*, W02429. https://doi.org/10.1029/2008WR006912

Klos, P. Z., Link, T. E., & Abatzoglou, J. T. (2014). Extent of the rain-snow transition zone in the western U.S. under historic and projected climate. *Geophysical Research Letters*, *41*, 4560–4568. https://doi.org/10.1002/2014GL060500

Liu, F., Williams, M. W., & Caine, N. (2004). Source waters and flow paths in an alpine catchment, Colorado Front Range, United States. *Water Resources Research*, *40*, W09401. https://doi.org/10.1029/2004WR003076

Longenecker, J., Bechtel, T., Chen, Z., Goldscheider, N., Liesch, T., & Walter, R. (2017). Correlating global precipitation measurement satellite data with karst spring hydrographs for rapid catchment delineation. *Geophysical Research Letters*, *44*, 4926–4932. https://doi.org/10.1002/2017GL073790

Maloszewski, P., Stichler, W., Zuber, A., & Rank, D. (2002). Identifying the flow systems in a karstic-fissured-porous aquifer, the Schneealpe, Austria, by modelling of environmental 18O and 3H isotopes. *Journal of Hydrology*, *256*(1-2), 48–59. https://doi.org/10.1016/S0022-1694(01)00526-1

McCallum, J. L., Cook, P. G., Berhane, D., Rumpf, C., & McMahon, G. A. (2012). Quantifying groundwater flows to streams using differential flow gaugings and water chemistry. *Journal of Hydrology*, *416-417*, 118–132. https://doi.org/10.1016/j.jhydrol.2011.11.040

McIntosh, J. C., Schaumberg, C., Perdrial, J., Harpold, A., Vázquez-Ortega, A., Rasmussen, C., et al. (2017). Geochemical evolution of the critical zone across variable time scales informs concentration-discharge relationships: Jemez River basin critical zone observatory. *Water Resources Research*, *53*, 4169–4196. https://doi.org/10.1002/2016WR019712

Meixner, T., Manning, A. H., Stonestrom, D. A., Allen, D. M., Ajami, H., Blasch, K. W., et al. (2016). Implications of projected climate change for groundwater recharge in the western United States. *Journal of Hydrology*, *534*, 124–138. https://doi.org/10.1016/j.jhydrol.2015.12.027

Miller, M. P., Tesoriero, A. J., Capel, P. D., Pellerin, B. A., Hyer, K. E., & Burns, D. A. (2016). Quantifying watershed-scale groundwater loading and in-stream fate of nitrate using high-frequency water quality data. *Water Resources Research*, *52*, 330–347. https://doi.org/10.1002/2015WR017753

Payn, R. A., Gooseff, M. N., McGlynn, B. L., Bencala, K. E., & Wondzell, S. M. (2009). Channel water balance and exchange with subsurface flow along a mountain headwater stream in Montana, United States. *Water Resources Research*, *45*, W11427. https://doi.org/10.1029/2008WR007644

Peterson, R. N., Santos, I. R., & Burnett, W. C. (2010). Evaluating groundwater discharge to tidal rivers based on a Rn-222 time-series approach. *Estuarine, Coastal and Shelf Science*, *86*(2), 165–178. https://doi.org/10.1016/j.ecss.2009.10.022

Pinault, J. L., Plagnes, V., Aquilina, L., & Bakalowicz, M. (2001). Inverse modeling of the hydrological and the hydrochemical behavior of hydrosystems: Characterization of karst system functioning. *Water Resources Research*, *37*(8), 2191–2204. https://doi.org/10.1029/2001WR900018

Rimmer, A., & Salingar, Y. (2006). Modelling precipitation-streamflow processes in karst basin: The case of the Jordan River sources, Israel. *Journal of Hydrology*, *331*(3-4), 524–542. https://doi.org/10.1016/j.jhydrol.2006.06.003

Ruehl, C., Fisher, A. T., Hatch, C., Huertos, M. L., Stemler, G., & Shennan, C. (2006). Differential gauging and tracer tests resolve seepage fluxes in a strongly-losing stream. *Journal of Hydrology*, *330*(1-2), 235–248. https://doi.org/10.1016/j.jhydrol.2006.03.025

Rugel, K., Golladay, S. W., Jackson, C. R., & Rasmussen, T. C. (2016). Delineating groundwater/surface water interaction in a karst watershed: Lower Flint River Basin, southwestern Georgia, USA. *Journal of Hydrology: Regional Studies*, *5*, 1–19.

Sauer, V. B., & Meyer, R. W. (1992). *Determination of error in individual discharge measurements* (p. 21). Norcross, Georgia: U.S. Geoloigcal Survey.

Schmadel, N. M., Neilson, B. T., & Kasahara, T. (2014). Deducing the spatial variability of exchange within a longitudinal channel water balance. *Hydrological Processes*, *28*(7), 3088–3103. https://doi.org/10.1002/hyp.9854

Spangler, L. E. (2001). Delineation of recharge in areas for karst springs in Logan Canyon, Bear River range, northern Utah, paper presented at U.S. Geological Survey karst interest group, U.S. Geological Survey Water Resources Investigations Report.

Spangler, L. E. (2011). Karst hydrogeology of the Bear River Range in the vicinity of the Logan River, Northern Utah, Paper Presented at Geological Society of America Rocky Mountain - Cordilleran Section Meeting, U.S. Geological Survey.

Taylor, S., Feng, X., Kirchner, J. W., Osterhuber, R., Klaue, B., & Renshaw, C. E. (2001). Isotopic evolution of a seasonal snowpack and its melt. *Water Resources Research*, *37*(3), 759–769. https://doi.org/10.1029/2000WR900341

Tennant, C. J., Crosby, B. T., & Godsey, S. E. (2015). Elevation-dependent responses of streamflow to climate warming. *Hydrological Processes*, *29*(6), 991–1,001. https://doi.org/10.1002/hyp.10203

White, W. B. (2002). Karst hydrology: Recent developments and open questions. *Engineering Geology*, *65*(2-3), 85–105. https://doi.org/10.1016/S0013-7952(01)00116-8

Winter, T. C. (1995). Recent advances in understanding the interaction of groundwater and surface water. *Reviews of Geophysics*, *33*(S2), 985–994. https://doi.org/10.1029/95RG00115